Vacuum ultraviolet-visible double resonance spectroscopy of NO. Observation of the high excited ns and nd Rydberg series

doi: 10.1063/1.456274

Vacuum ultraviolet–visible double resonance spectroscopy of NO. Observation of the high excited *ns* and *nd* Rydberg series

Asuka Fujii, Takayuki Ebata, and Mitsuo Ito
Department of Chemistry, Faculty of Science, Tohoku University, Sendai 980, Japan

(Received 30 December 1988; accepted 6 March 1989)

The two-color double resonance multiphoton ionization and fluorescence dip spectra due to the transitions from various rotational levels of the $D\,^2\Sigma^+$ ($v = 1$) state of NO to its high Rydberg states have been measured. Coherent vacuum ultraviolet (VUV) light generated by four wave mixing in Hg was used in the first excitation step. The $ns(v = 1)$ and $nd(v = 1)$ Rydberg series with $7 \leq n \leq 32$ were observed. The rotational analysis for the d Rydberg series indicates that only the Π^- component appears in the MPI spectra. A large dependence of the rotational constant upon n for the nd Π^- Rydberg states was found and interpreted in terms of $d\Pi^- - d\Delta^-$ mixing. An anomalous intensity distribution was also found for the rotational branches of the ns Rydberg states in the transition from the $D\,^2\Sigma^+$ state. The anomaly is explained by the ns–$(n-1)d$ mixing.

I. INTRODUCTION

Nitric oxide has been a pet molecule of spectroscopists and subject to numerous studies for many years. Among them, the high resolution vacuum–ultraviolet abosorption studies by Miescher and co-workers[1–10] had elucidated detailed features of this molecule in a wide energy range. In general, the detailed study of high Rydberg states of a molecule is very difficult by ordinary one-photon absorption spectroscopy because of spectral congestion due to overlapping of various transitions. To explore these states, two-color multiphoton spectroscopy has been found to be very useful for its high selectivity.[11–18] Using this technique, the high $ns(v = 0,1)$,$np(v = 0,1)nd(v = 0)$, and $nf(v = 1)$ Rydberg series of NO have been observed via the $A\,^2\Sigma^+$ (Refs. 11–15) and $C\,^2\Pi$ (Refs. 16–18) states, and the detailed analysis has been performed. But there are still many unexplained phenomena. One of these is concerned with the observation of the d Rydberg state ($v = 1$).

In previous papers,[11–13] we have reported the two-color multiphoton-ionization (MPI) spectra of NO molecule via the $A\,^2\Sigma^+(3s\sigma)(v = 1)$ state, and observed the ns, np, and $nf(v = 1)$ Rydberg series. The appearance of the np series in the transition from the $3s\sigma$ state is readily understood from the selection rule of $\Delta l = \pm 1$. On the other hand, the appearance of the ns and nf series was interpreted as a result of the admixture of p and d characters in the $A\,^2\Sigma^+(3s\sigma)$ state.[19–21] If we admit the admixture, we also expect the appearance of d Rydberg series, which results from the small p character in the A state. However, in spite of the strong transition to the high ns Rydberg series, no d Rydberg series was found. The absence of the d Rydberg series might be due to the predissociation of the d Rydberg state ($v = 1$) molecule or to the interference effect originated from $s - d$ mixing. We have no reasonable explanation for the above phenomenon as yet.

The high excited nd Rydberg states of $v = 0$ has been observed by Seaver *et al.*,[16] Fredin *et al.*,[17] and Pratt[18] in their two-color MPI measurements via the $C\,^2\Pi$ state and was analyzed in detail especially by Fredin *et al.* But, the nd Rydberg states of $v = 1$ have never been observed. The purpose of the present study was to observe these states. The experimental scheme is depicted in Fig. 1. We have observed the high Rydberg states of NO above the ionization limit by using the $D\,^2\Sigma^+(v = 1)$ state as an intermediate state in the two-color MPI or fluorescence dip measurement. The $D\,^2\Sigma^+$ state which we chose as the intermediate state is the $3p\sigma$ Rydberg state, therefore strong transition to the d Rydberg state is expected. Due to the similarity of the potential curves of the Rydberg states, the Franck–Condon factor is large for the transition from the $v = 1$ intermediate state to the $v = 1$ Rydberg state. Thus, we expect the strong appearance of the nd Rydberg states belonging to $v = 1$ by employing the $D\,^2\Sigma^+(v = 1)$ state as an intermediate state. The selection of the $D\,^2\Sigma^+$ state has also an advantage to simplify the transition and to perform parity selected excitation.

The $D\,^2\Sigma^+(v = 1)$ state lies at 55 550 cm^{-1}, that is, in the vacuum ultraviolet region. To excite the molecule to the D state with UV laser light, the two-photon excitation is required, then we have to increase laser power. In that case, it is difficult to avoid subsequent one-photon absorption

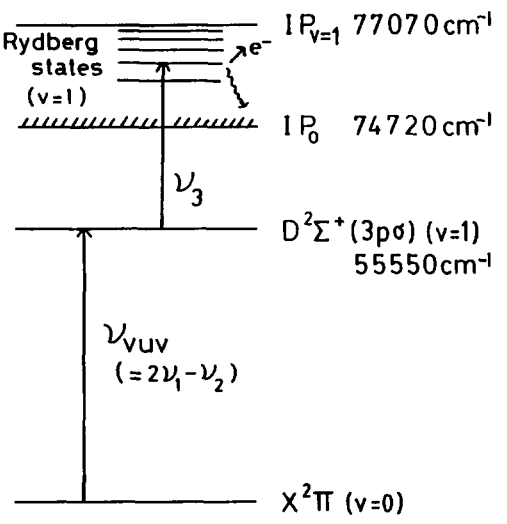

FIG. 1. Schematic diagram of VUV–visible double resonance excitation of NO.

 0021-9606/89/126993-07$02.10

from the D state, which produces a strong ionization signal. This situation makes the double reasonance experiment very difficult. To overcome the difficulty, we used coherent vacuum–ultraviolet laser light generated by four wave mixing in Hg vapor.[22,23] The VUV light generated by different frequency mixing of two laser lights ($\nu_{VUV} = 2\nu_1 - \nu_2$) excites NO molecules in a supersonic free jet to a specific rovibronic level of the D state by one-photon absorption. Tunable laser light of ν_3 is used to excite the D state molecule to a higher Rydberg state lying above the ionization limit. The NO molecule in the Rydberg state thus prepared immediately autoionizes and produces the ion. By this double resonance method, we could observe intense transitions to both the *ns* and *nd* Rydberg states from the $D\,^2\Sigma^+$ state. A detailed rotational analysis will be shown for the 8*d* Rydberg state taken as an example. It was found that the rotational constant of the *nd* Rydberg state increases with an increase of the principal quantum number n. As to the transition to the $ns\,^2\Sigma^+$ state, the intensity distribution in the P and R branches was also found to vary with n.

We also observed the same transitions from the $D\,^2\Sigma^+$ state to the higher Rydberg states by fluorescence dip spectroscopy in which the transitions are detected by the dip of the fluorescence from the $D\,^2\Sigma^+$ state. It was found that the relative intensities of the bands in the fluorescence dip spectrum are different from those in the MPI spectrum. The difference provides us with information on the predissociation of the high excited Rydberg molecule, which supplements the results reported in a previous paper.[18]

II. EXPERIMENTAL

A Nd–YAG laser (Quantel YG 581-10) pumped three dye lasers simultaneously. The first dye laser (ν_1) (Quantel TDL 50 with Rhodamine 6G dye) was pumped by second harmonic (532 nm) of the YAG laser. Its output was frequency doubled and the frequency was fixed on the two-photon transition of $6d\,^1D_2$–$6s\,^1S_0$ of Hg (280.29 nm). The second and third dye lasers (ν_2, ν_3) were pumped by third harmonic (355 nm) of the YAG laser. The output of the second dye laser (Molectron DL14 with DCM dye) was introduced coaxially with the ν_1 laser beam by a dichroic mirror. The two laser beams were focused into a stainless steel oven containing Hg vapor and Kr buffer gas. The oven was the heat-pipe-type and the same as that described by Tsukiyama *et al.*[24] The coherent VUV light was generated by difference frequency mixing ($\nu_{VUV} = 2\nu_1 - \nu_2$) in the oven. The best condition for this mixing process was described by Hilbig *et al.*[23] The generated VUV light was introduced into a vacuum chamber through a MgF_2 window to excite NO in a supersonic free jet. The NO gas seeded in 2 atm He was expanded through a pulsed nozzle of 0.4 mm orifice into the vacuum chamber (background pressure $= 2\times10^{-5}$ Torr). The wavelength of the VUV light was fixed to a selected rotational line of the $D\,^2\Sigma^+ \leftarrow X\,^2\Pi$ (1,0) transition. The third laser light (ν_3) (Molectron DL14 with Coumarin 480,500 dyes) was introduced into the chamber counterpropagated to the VUV light and was scanned to probe the high Rydberg states. The ions produced by autoionization of the high Rydberg state molecules were brought into a detector chamber by a repeller at an electric field of 12 V/cm and were detected by an electron multiplier (Murata ceratron). The signal was amplified by a current amplifier (Keithly 427) and averaged by a boxcar integrator (Parr model No. 4402/4420). In the fluorescence dip measurement, the fluorescence from the $D\,^2\Sigma^+$ state to the ground state was monitored at right angles to both the laser beams by a solar blind photomultiplier (Hamamatsu R166UH) after passing through an interference filter centered at 235 nm.

III. RESULTS AND DISCUSSION

A. Gross feature of the spectra and rotational analysis of the 8*d* Rydberg state

Figure 2 shows the MPI spectrum of the $D\,^2\Sigma^+ \leftarrow X\,^2\Pi$ (1,0) transition of NO which was obtained by excitation of the molecule to the D state by one-photon absorption of the tunable VUV light followed by ionization of the D state molecule by the absorption of the UV light of a fixed frequency (ν_1). The VUV light was weak enough to avoid the multiphoton ionization by this light alone. Since the NO molecules in a jet are well cooled, the individual rotational lines are resolved as seen in the figure. The rotational temperature was estimated to be 14($\pm$ 3) K, and the rotational levels were observed up to $N = 4$. We chose an isolated rotational line belonging to P_{11} or R_{21} branch for the excitation to the selected rotational level in $D\,^2\Sigma^+(v = 1)$ with ν_{VUV}.

Figure 3 shows the two-color MPI spectrum obtained by selecting the $J = 1.5$ ($N = 1$) level of the $D\,^2\Sigma^+(v = 1)$ state with the VUV light and by scanning the frequency of the probing visible laser light of ν_3. Two Rydberg series, both of which converge to the vertical ionization threshold ($NO^+, v = 1$) at 77 070 cm^{-1}($\nu_3 + \nu_{VUV}$), clearly appear in the spectrum. One of the series coincides with the high *ns* Rydberg series ($v = 1$) which was observed in the two-color MPI spectrum via the $A\,^2\Sigma^+$ state. Therefore, it can be assigned to the *ns* Rydberg series ($v = 1$). On the other hand, another series does not coincide with the *np* or *nf* series which appears in the same two-color MPI spectrum via the

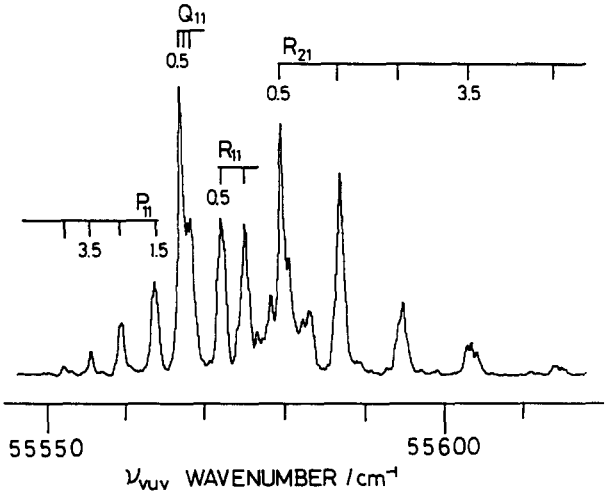

FIG. 2. (VUV + UV) MPI spectrum of the $D\,^2\Sigma^+ \leftarrow X\,^2\Pi$ (1–0) band of NO in a supersonic free jet.

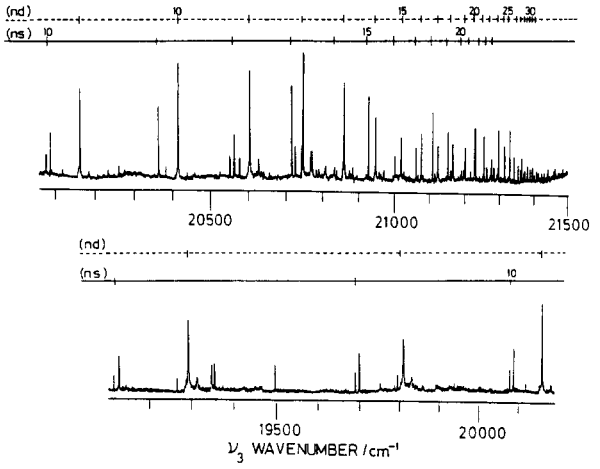

FIG. 3. Two-color MPI spectrum of NO due to the transition from the $D\,^2\Sigma^+(v=1), J=1.5(N=1)$ level.

A state.[12,13] This series can be assigned to the high nd Rydberg series ($v=1$) because of its strong intensity as expected for the transition from the intermediate $D\,^2\Sigma^+(3p\sigma)$ state. The quantum defect of the series is -0.046, supporting the above assignment. In addition to the high ns and nd series, a very weak f Rydberg series and a few unassigned peaks were observed in the region from $n=7$ to $n=10$. The transitions to the high nd Rydberg states are easily staturated by ordinary laser power. Under the unsaturated condition, the MPI intensity of the nd state is about 5 times stronger than that of the corresponding ns state. According to the calculations by Kaufmann *et al.*[19] and by Viswanathan *et al.*,[21] the $D\,^2\Sigma^+$ Rydberg state is of almost pure p character. Therefore, the strong intensity of the high ns and nd series and very weak intensity of the f series in the spectrum taken via the D state are readily understood. This is in contrast to the spectrum taken via the $A\,^2\Sigma^+(3s\sigma)$ state, where the high ns and nf series appeared strongly against the expectation. In the present measurement, we observed the nd Rydberg states ($v=1$) from $n=7$ to $n=32$ and the ns Rydberg states ($v=1$) from $n=8$ to $n=24$. The energies of the observed nd Rydberg states are listed in Table I.

The rotational energy levels belonging the the ns and nd Rydberg states can be obtained from the two-color MPI spectra measured by exciting various rotational levels in the $D\,^2\Sigma^+(v=1)$ state with the VUV light. Figure 4 shows the two-color MPI spectra due to the transitions from various rotational levels in the D state to the $9s(v=1)$ and $8d(v=1)$ Rydberg states. Here, J denotes the total angular momentum and N the total angular momentum apart from spin in the D state which belongs to Hund's case (b). The rotational analysis of the ns Rydberg states was already described in previous papers.[12,13] Two peaks of the s Rydberg state in the spectrum of $N>0$ correspond to the transitions $\Delta N=\pm 1$. The transition to the d Rydberg state from the D state gives a sharp strong peak when $N\geqslant 1$ in the D state. Weak peaks on the lower frequency side of the d Rydberg peaks in the spectra of $N=1$ and 2 are assigned to the f Rydberg states. In the spectrum of $N=0$, only a weak and broad band can be seen instead of the strong peak. The rea-

TABLE I. Energy of the d Rydberg series measured by pumping the $J=1.5$ ($N=1$) level in the $D\,^2\Sigma^+$, $v=1$ state (55 573.3 cm^{-1}).

n	Energy/cm^{-1}
7	74 866.5
8	75 381.8
9	75 735.8
10	75 988.9
11	76 179.1
12	76 320.3
13	76 432.0
14	76 520.2
15	76 592.3
16	76 650.6
17	76 698.0
18	76 739.2
19	76 774.8
20	76 804.0
21	76 828.3
22	76 850.0
23	76 869.7
24	76 887.1
25	76 902.1
26	76 915.2
27	76 927.1
28	76 937.7
29	76 947.3
30	76 954.6
31	76 962.6
32	76 969.4

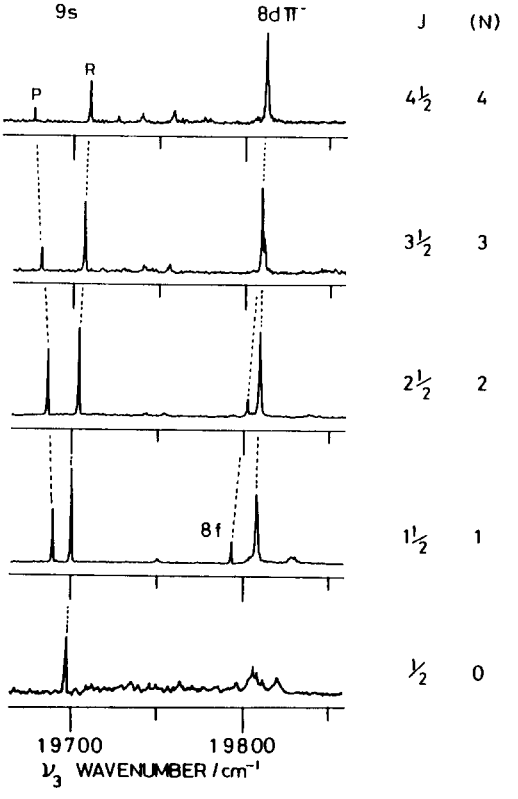

FIG. 4. Two-color MPI spectra due to the transitions from various rotational levels of the $D\,^2\Sigma(v=1)$ state to the $9s(v=1)$, $8d(v=1)$ states. J and N denote the rotational quantum number of the D state.

son for this will be discussed later. For the assignment of the strong peak of 8*d*, we need additional information beside the spectra of Fig. 4. For this purpose, we measured the two-color MPI spectrum due to the transition from the $C\,^2\Pi$ ($v=1$) to the 8*d* Rydberg states. Since the $C\,^2\Pi$ state is the $3p\pi$ Rydberg state, we can expect strong appearance of the *nd* Rydberg states in the spectrum. Figure 5 shows the two-color MPI spectra due to the transitions to the 8*d* Rydberg state from various rotational levels in the *C* state. The $C\,^2\Pi$ state lies only 900 cm^{-1} below the $D\,^2\Sigma^+$ state and can be easily excited by the VUV light. In the transition from the $C\,^2\Pi(v=1)$ state, the two components of the 8*d* Rydberg state, $8d\pi$ and $8d\delta$, appear in the spectra and they can be assigned by analogy with the analysis of the two-color MPI spectra due to the transition $nd \leftarrow C\,^2\Pi$ (0,0) made by Fredin *et al.*[17] In particular, the π component can be unequivocally assigned by the fact that only two lines (Q and R) were observed in the transition from $N=1$ level in the $D\,^2\Sigma^+$ ($v=1$) state, but three lines (P,Q, and R for $\Delta N=-1,0$, and 1) in the transition from the level of $N>1$. It was found that absolute frequencies ($\nu_3+\nu_{vuv}$) of the observed Q lines exactly coincide with those of the strong 8*d* peaks in the two-color spectra via $D\,^2\Sigma^+$ shown in Fig. 4. Therefore, the individual 8*d* peaks in the spectra due to the transitions from $D\,^2\Sigma^+(1,1)$ are assigned to the Q branch ($\Delta N=0$) of the $d\pi$ component. Moreover by considering the parity selection rule,[25] we can specify the symmetry of the *d* Rydberg state. Figure 6 shows a schematic diagram of the transitions. Due to the one-photon parity selection rule $+\leftrightarrow-$, P and R

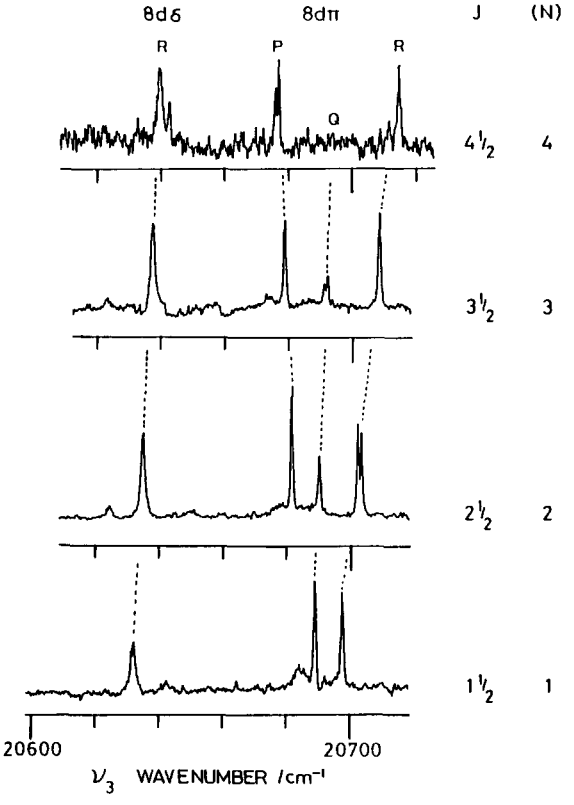

FIG. 5. Two-color MPI spectra due to the transitions from various rotational levels of the $C\,^2\Pi(v=1)$ state to the 8*d* Rydberg state.

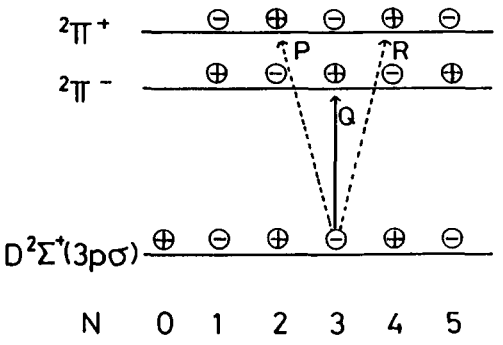

FIG. 6. Parity selectivity of the one-photon allowed $^2\Pi \leftarrow {}^2\Sigma$ transition. The solid line (Q branch) shows the transition to the Π^- component, and dashed to the Π^+ component.

branches appear for the transition to the Π^+ component, and Q branch for the Π^- component. The fact that only the Q branch appears in the transition from the D state shows that the *d* Rydberg state is assigned to $d\Pi^-$. This assignment becomes possible because of the parity selected excitation from the $D\,^2\Sigma^+$ state. The absence of $d\,\Sigma^+$ and $d\,\Pi^+$ components will be discussed later.

B. *l* uncoupling in the high *d* Rydberg states

In general, high Rydberg states of a diatomic molecule are characterized by *l* uncoupling, that is, transition from Hund's case(b) to case(d).[25] With the increase of principal quantum number, orbital angular momentum becomes more and more uncoupled with the molecular axis. As a result, the Σ, Π, and Δ components which are defined by the projection of *l* onto the molecular axis (λ), mix each other (*l* uncoupling). The rotational wave function of pure case(b) is given by [13,26]

$$\Phi_\Lambda^{\rm rot} = 2^{-1/2}(|lN,\lambda;l,\lambda\rangle \pm |lN,-\lambda;l,-\lambda\rangle), \qquad (1)$$

where Λ is the absolute value of λ. The rotational part of the Hamiltonian is given by

$$\hat{H}_{\rm rot} = B_v\{\hat{N}^2 - \hat{N}_z^2 + \hat{l}^2 - \hat{l}_z^2 - (\hat{N}_+\hat{l}_{-+}\hat{l}_+\hat{N}_-)\}. \qquad (2)$$

From the Eqs. (1) and (2), the energy matrix in terms of the case(b) basis set is obtained as shown in Table II. We see immediately from the form of the matrix that the Λ^+ components (Σ^+,Π^+ and Δ^+) do not interact with the Λ^- components (Π^- and Δ^-). This is the parity selection rule for

TABLE II. Energy matrix of *d* Rydberg state ($l=2$). $H_\Lambda = T_\Lambda^{cv} + B_v^+[N(N+1)+6-2\Lambda^2]$, $H_{\Delta\Pi} = H_{\Pi\Delta} = 2B_v^+[(N-1)(N+2)]^{1/2}$, $H_{\Pi\Sigma} = H_{\Sigma\Pi} = 2B_v^+[3N(N+1)]^{1/2}$.

	(Λ=2) Δ^+	(Λ=1) Π^+	(Λ=0) Σ^+	(Λ=1) Π^-	(Λ=2) Δ^-
Δ^+	H_Δ	$H_{\Delta\Pi}$	0		
Π^+	$H_{\Pi\Delta}$	H_Π	$H_{\Pi\Sigma}$	0	
Σ^+	0	$H_{\Sigma\Pi}$	H_Σ		
Π^-				H_Π	$H_{\Pi\Delta}$
		0			
Δ^-				$H_{\Delta\Pi}$	H_Δ

perturbation.[25] This result is very important in the analysis of the spectra obtained in this work.

The l uncoupling provides several characteristic features to the spectra of NO. One of these is the anomalous behavior of the rotational constant of the high Rydberg state. Based on the rotational levels of the d Π^- Rydberg state, the rotational constant for the Rydberg state of each principal quantum number is obtained from a plot of the energy levels vs $N(N+1)$. Figure 7 shows such a plot for the $8d\ \Pi^-$ state as an example. The rotational constants obtained for various $nd\ \Pi^-$ Rydberg states are listed in Table III. Figure 8 shows a plot of the rotational constant vs principal quantum number n. The rotational constant increases rapidly with the increase of n. A similar change of rotational constant was found also for the high ns Rydberg states as was reported by Anezaki *et al.*[13] and by Miescher.[10] In the case of the $ns\ ^2\Sigma^+$ states, the rotational constant decreases with the increase of n. Such a change of rotational constant arises from the change of rotational energy caused by l uncoupling.[10,13,17,27] The anomalous behavior of the rotational constant of the $ns\ ^2\Sigma^+$ state was explained as a consequence of the interaction between the $(n-1)d\ \Pi^+$ state and the $(n-1)d\ \Sigma^+$ state which is mixed with the $ns\ \Sigma^+$ state. However, as described above, this interaction does not affect the $d\ \Pi^-$ component. The $d\ \Pi^-$ component can interact only with the $d\ \Delta^-$ component by l uncoupling. From the energy matrix in the Table II, the term value of the perturbed $d\ \Pi^-$ component is given by

$$T_{d\Pi^-} = \tfrac{1}{2}(H_{\Pi^-} + H_{\Delta^-}) + \tfrac{1}{2}\sqrt{(H_{\Pi^-} - H_{\Delta^-})^2 + 4H_{\Pi\Delta}^2}. \quad (3)$$

The unperturbed energies of the $d\ \Pi^-$ and $d\Delta^-$ states in terms of the quantum defects are

TABLE III. Rotational constants of the $d\ \Pi^-$ Rydberg series.

n	B_{obs}/cm^{-1}	B_{calc}/cm^{-1}
7	2.10	2.11
8	2.20	2.18
9	2.25	2.25
10	...	2.32
11	2.34	2.38
12	2.37	2.43
13	2.43	2.48

$$H_{\Pi^-} = \mathrm{IP}_v - \frac{R}{(n-\delta\Pi^-)^2} + B_v^+ N(N+1), \quad (4)$$

$$H_{\Delta^-} = \mathrm{IP}_v - \frac{R}{(n-\delta_{\Delta^-})^2} + B_v^+ N(N+1), \quad (5)$$

where IP_v is the vertical ionization potential corresponding to the energy of the $v=1$ state of the ion. B_v^+ is the rotational constant of the NO^+ ion in the $v=1$ state. R is the Rydberg constant, and δ_{Π^-} and δ_{Δ^-} are the quantum defects. We calculated the energy terms of Eq. (3) up to $N=5$ for each n by using $B_v^+ = 1.97\ cm^{-1}$, $\delta_{\Pi^-} = -0.045$, $\delta_{\Delta^-} = 0.112$,[28] and $R = 109\,735.3\ cm^{-1}$. Then, the value of B_v was calculated by the first-order regression analysis with respect to $N(N+1)$. The calculated B_v are listed in Table III and also shown by the curve in Fig. 8. The good agreement between the observed and calculated values indicates

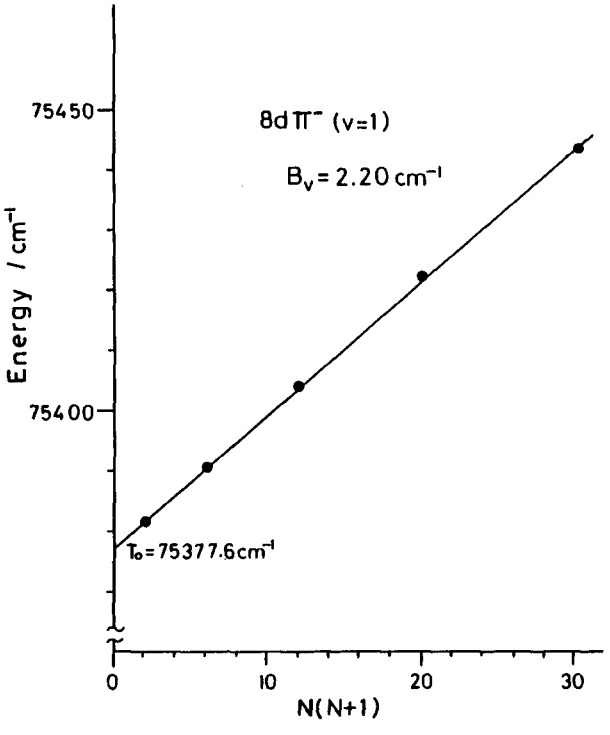

FIG. 7. Plot of the rotational energy levels of the $8d\ \Pi^-$ component vs $N(N+1)$.

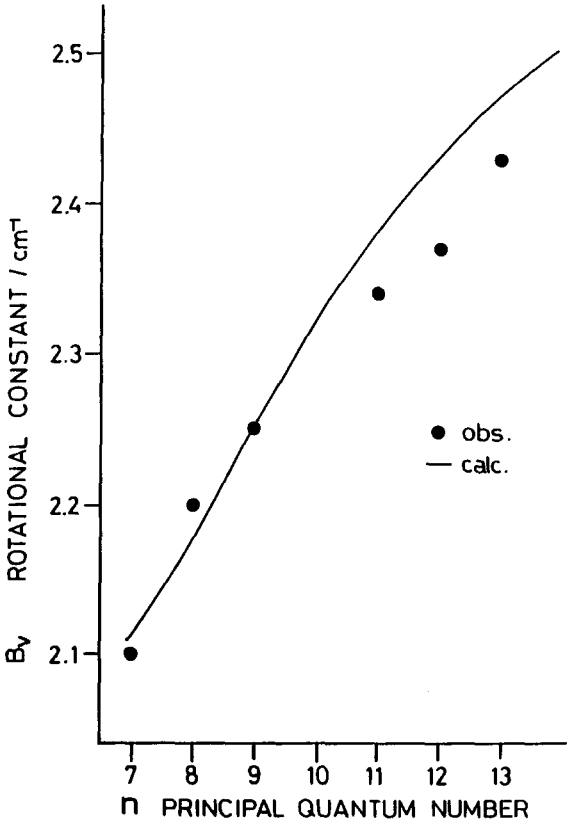

FIG. 8. Plot of rotational constant of the $d\ \Pi^-$ component vs n.

that the n dependence of the rotational constant arises from the interaction of the $d\,\Pi^-$ state with the $d\,\Delta^-$ state.

l uncoupling causes also an anomalous intensity distribution. The intensity distribution of the rotational branches in the transitions to the high ns Rydberg states from the $D\,^2\Sigma^+$ state is quite different for different principal quantum number n. For $n = 7$–10, two peaks corresponding to the P and R branches appear in the spectra as is seen as an example for the 9s Rydberg state in Fig. 4. However, for higher n ($= 11$–24) the P branch is missing completely as is shown in Fig. 9.

Huber[29] had reported a similar missing of the P branch line in the emission spectrum due to the transition from the $H\,^2\Sigma^+(3d\sigma)$ to the $D\,^2\Sigma^+$ state. He interpreted this to be a result of the interference effect between the $H\,^2\Sigma^+(3d\sigma)$ state and the nearby $H'^2\Pi(3d\pi)$ state which mix by l uncoupling. The transition moment A for the $H\,^2\Sigma^+ \rightarrow D\,^2\Sigma^+$ transition is given by

$$A = CA_{d\sigma} + C'A_{d\pi}, \tag{6}$$

where $A_{d\sigma}$ and $A_{d\pi}$ are unperturbed transition moments from the $3d\sigma$ and $3d\pi$ states to the $D\,^2\Sigma^+$ state, and C and C' are coefficients. The absolute values of the two terms of Eq. (6) are nearly equal. But, the two terms have opposite sign for P branch line but the same sign for R branch line. Consequently the transition moment for the P branch line almost vanishes, and only the R branch line is observed.

The absence of the P branch line in the high ns Rydberg states with $n \geqslant 12$ in the transition from the $D\,^2\Sigma^+$ state may also be explained by a similar interference effect between $d\sigma$ and $d\pi$ states, which is caused by the l uncoupling. The ns Rydberg orbital of NO is known to strongly mix with $(n = 1)d\sigma$ orbital due to the nonspherical field of the core.[27] The $(n - 1)d\sigma$ character in the ns Rydberg state increases with the increase of n because the energy difference between the ns and $(n = 1)d\sigma$ states decreases with the increase of n. As a result of the increase of the $d\sigma$ character, the intensity of the P branch line becomes weak with the increase of n and finally vanishes for $n \geqslant 12$ by the interference effect similar to that considered by Huber.

C. The two-color fluorescence dip spectra

Because of the parity selection rule, transition to the $d\,\Pi^-$ component from the $N = 0$ level of the $D\,^2\Sigma^+$ state is prohibited (see Fig. 6). However, in the two-color MPI spectrum due to the transition from the $N = 0$ level in the $D\,^2\Sigma^+(v = 1)$ state (Fig. 4), we observed broad and weak peaks around the position of 8d. These peaks should be assigned to the states other than the $d\,\Pi^-$ state. A similar broad and weak MPI peak is also seen near the sharp peak of the $nd\,\Pi^-$ component in the spectrum due to the transition from $N \geqslant 1$ level in the D state. The presence of the broad peak around $d\,\Pi^-$ is more clearly seen in the two-color fluorescence dip spectra which are shown in Fig. 10. The figure shows the fluorescence dip spectra of the $8d \leftarrow D\,^2\Sigma^+(1,1)$ transition from the $N = 0$ and $N = 1$ levels in the $D\,^2\Sigma^+(v = 1)$. These dip spectra were obtained by monitoring the fluorescence from the $D\,^2\Sigma^+$ state. Note that because of large power of the probing laser light (ν_3) the transition to the 8d Rydberg state is saturated. The depth of the broad dip is almost the same order in magnitude as that of the $8d\Pi^-$ component. Since the depth of the fluorescence dip directly reflects the absorption cross section, the transition moment associated with the broad dip will be almost the same as that associated with the $d\Pi^-$ state. The broadness suggests that the state associated with the broad dip has a very fast relaxation process such as predissociation. The candidates for such states are the $d\,\Sigma^+$ and the $d\,\Pi^+$ components. If the broad peak is assigned to the $d\,^2\Sigma^+$ and $d\,^2\Pi^+$ components, the interacting dissociative state should be of Σ^+ or Π^+ symmetry by noting the parity selection rule for perturbation.

Finally, we would like to make a comment on the results of the two-color MPI spectrum via the $A\,^2\Sigma^+(3s\sigma)$ state reported in previous papers[11–13] and their relation with the present study. In previous papers, we showed that the MPI spectrum from the $A\,^2\Sigma^+(3s\sigma)$ state exhibits the high ns, np, and nf Rydberg series. The appearance of the high ns and nf states which is against the $\Delta l = \pm 1$ selection rule was interpreted as a result of the admixture of the p and d characters in the $A\,^2\Sigma^+(3s\sigma)$ state. If we admit the admixture, we also

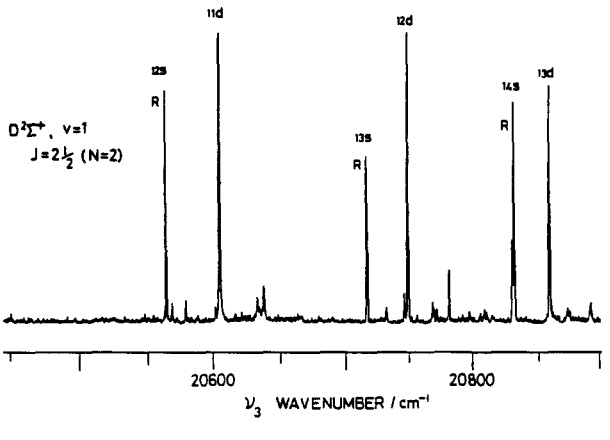

FIG. 9. Two-color MPI spectrum for the transition from the $D\,^2\Sigma^+$ ($v = 1$), $N = 2$ level. The P branches of the transition to the 12s, 13s, and 14s states are absent.

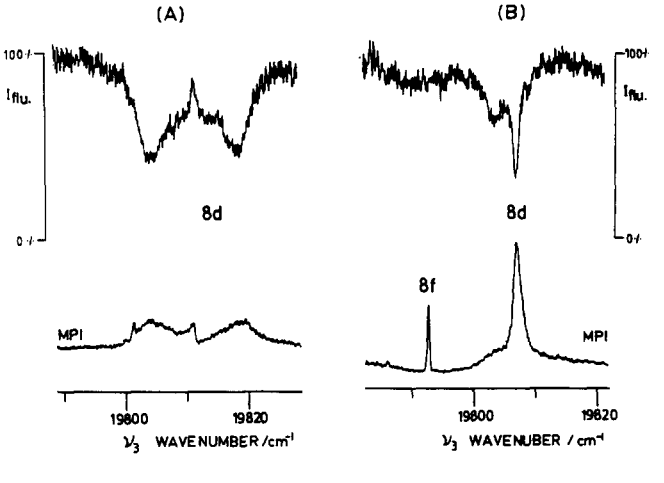

FIG. 10. Two-color MPI and fluorescence dip spectra due to the transition from the $D\,^2\Sigma^+(v = 1)$, (A) $N = 0$, (B) $N = 1$ level to the 8d Rydberg region.

expect the appearance of the high *nd* Rydberg series besides *ns*, *np*, and *nf* series in the two-color MPI spectrum via the $A\,^2\Sigma^+$ state. However, we could not find even trace of the *nd* Rydberg series. In addition, the *p* character in the $A\,^2\Sigma^+$ state is estimated to be less than 1%.[19–21] This small *p* character seems to be contrary to the strong appearance of the high *ns* states in the MPI spectrum from the $A\,^2\Sigma^+(3s\sigma)$ state. This is a question we have had since then.

In the present work we measured the two-color MPI spectrum via the $3p\sigma$ ($D\,^2\Sigma^+$) state and observed the transitions to the high *ns* and *nd* Π^- states with the nearly equal intensities. Taking into account this result, the *p* character in the $A\,^2\Sigma^+(3s\sigma)$ state should give the *ns* and *nd* Rydberg series with comparable intensities in the two-color MPI spectrum. Therefore, even if $A\,^2\Sigma^+(3s\sigma)$ has a small *p* character, this *p* character is not directly involved in the observation that the *ns* series appears strongly and the *nd* series is absent. Then, the reason which explains the observation should be found in the final state of the transition instead of the intial $A\,^2\Sigma^+$ state. If we assume a considerable *p* character in the high *ns* Rydberg states, the strong appearance of these *ns* states can be explained. Moreover, the absence or extremely weak intensity of the *nd* series is also understood by this assumption. The calculation by Viswanathan *et al.*[21] shows that the $4s\sigma$ and $5s\sigma$ have more *p* character than that of the $A\,^2\Sigma^+(3s\sigma)$ state, supporting the assumption. Therefore, we conclude that the high *ns* Rydberg state has a considerable *p* character, which makes the forbidden $ns \leftarrow A\,^2\Sigma^+(3s\sigma)$ ($\Delta l = 0$) transition strongly allowed.

IV. CONCLUSIONS

The two-color double resonance MPI and fluorescence dip spectra of NO due to the transitions from the $D\,^2\Sigma^+(v=1)$ state have been measured, and the $ns(v=1)$ and $nd(v=1)$ Rydberg series with high principal quantum number *n* have been observed. The transition was well characterized by the normal $\Delta l = \pm 1$ selection rule, proving the pure $p\sigma$ character of the $D\,^2\Sigma^+$ state. The rotational analysis showed that the *nd* Rydberg state appearing in the MPI spectrum is assigned to the $d\,\Pi^-$ component. The other components, $d\,\Sigma^+(v=1)$ and $d\,\Pi^+(v=1)$, seem to appear in the fluorescence dip spectra and they are broadened by predissociation. A large dependence of the rotational constant upon principal quantum number for the *nd* Π^- component was found and was explained based on the *l* uncoupling. Anomalous intensity of the rotational branch of the *ns* Rydberg state in the transition from the $D\,^2\Sigma^+$ state as interpreted as a result of interference effect between the $d\sigma$ character in the *s* Rydberg state and the $d\pi$ state.

The present work is the first demonstration of the two-color MPI measurement using coherent VUV light. This shows validity of application of the coherent VUV light generated by frequency mixing for the study of high excited molecule.

ACKNOWLEDGMENTS

We are grateful to Dr. K. Tsukiyama for helpful advice on the heat pipe oven. We also thank T. Amano and N. Hosoi for experimental assistance.

[1] A. Lagerqvist and E. Miescher, Helv. Phys. Acta **31**, 221 (1958).
[2] A. Lagerqvist and E. Miescher, Can. J. Phys. **40**, 352 (1962).
[3] K. P. Huber and E. Miescher, Helv. Phys. Acta **36**, 257 (1963).
[4] A. Loftus and E. Miescher, Can. J. Phys. **42**, 848 (1964).
[5] K. Dressler and E. Miescher, Astrophys. J. **141**, 1266 (1965).
[6] A. Lagerqvist and E. Miescher, Can. J. Phys. **44**, 1525 (1966).
[7] E. Miescher, J. Mol. Spectrosc. **20**, 130 (1966).
[8] Ch. Jungen and E. Miescher, Can. J. Phys. **46**, 987 (1968).
[9] Ch. Jungen and E. Miescher, Can. J. Phys. **47**, 1769 (1969).
[10] E. Miescher, Can. J. Phys. **54**, 2074 (1976).
[11] T. Ebata, Y. Anezaki, M. Fujii, N. Mikami, and M. Ito, J. Phys. Chem. **87**, 4773 (1983).
[12] Y. Anezaki, T. Ebata, N. Mikami, and M. Ito, Chem. Phys. **89**, 103 (1984).
[13] Y. Anezaki, T. Ebata, N. Mikami, and M. Ito, Chem. Phys. **97**, 153 (1985).
[14] D. T. Biernacki, S. D. Colson, and E. E. Eyler, J. Chem. Phys. **88**, 2099 (1988).
[15] D. T. Biernacki, S. D. Colson, and E. E. Eyler, J. Chem. Phys. **89**, 2599 (1988).
[16] M. Seaver, W. A. Chupka, D. Colson, and D. Gauyacq, J. Phys. Chem. **87**, 2226 (1983).
[17] S. Fredin, D. Gauyacq, M. Horani, Ch. Jungen, G. Lefever, and F. Musnou-Seeuws, Mol. Phys. **60**, 825 (1987).
[18] S. T. Pratt, Chem, Phys. Lett. **151**, 131 (1988).
[19] K. Kaufmann, C. Nager, and M. Jungen, Chem. Phys. **95**, 385 (1985).
[20] S. N. Dixt, D. L. Lynch, V. McKoy, and W. M. Huo, Phys. Rev. A **32**, 1267 (1985).
[21] K. S. Viswanathan, E. Sekreta, E. R. Davison, and J. P. Reilly, J. Phys. Chem. **90**, 5078 (1986).
[22] J. W. Hepbern, Israel J. Chem. **24**, 273 (1984).
[23] R. Hilbig and R. Wallenstein, IEEE. J. Quantum Electron **QE19**, 1759 (1983).
[24] K. Tsukiyama, T. Munakata, M. Tsukakoshi, and T. Kasuya, Chem. Phys. **121**, 55 (1988).
[25] G. Herzberg, *Molecular Spectra and Molecular Structure, Vol. I, Spectra of Diatomic Molecules* (Van Nostrand, New York, 1950).
[26] I. Kovacs, *Rotational Structure in the Spectra of Diatomic Molecules* (American Elsevier, New York, 1969).
[27] Ch. Jungen, J. Chem. Phys. **53**, 4168 (1970).
[28] Observed value for the 8 $d\Delta$ state in this experiment.
[29] M. Huber, Helv. Phys. Acta **37**, 329 (1964).